Structural basis for abrogated binding between staphylococcal enterotoxin A superantigen vaccine and MHC-IIα

HEIKE I. KRUPKA,[1,4] BRENT W. SEGELKE,[1,4] ROBERT G. ULRICH,[2] SABINE RINGHOFER,[1] MARK KNAPP,[3] AND BERNHARD RUPP[1]

[1]Lawrence Livermore National Laboratory, Macromolecular Crystallography, Biology and Biotechnology Research Program, University of California, Livermore, California 94551, USA
[2]Army Medical Research Institute of Infectious Diseases, Laboratory of Molecular Immunology, Frederick, Maryland 21702, USA
[3]Roche Bioscience, Palo Alto, California 94304, USA

(RECEIVED October 1, 2001; FINAL REVISION November 14, 2001; ACCEPTED November 26, 2001)

Abstract

Staphylococcal enterotoxins (SEs) are superantigenic protein toxins responsible for a number of life-threatening diseases. The X-ray structure of a staphylococcal enterotoxin A (SEA) triple-mutant (L48R, D70R, and Y92A) vaccine reveals a cascade of structural rearrangements located in three loop regions essential for binding the α subunit of major histocompatibility complex class II (MHC-II) molecules. A comparison of hypothetical model complexes between SEA and the SEA triple mutant with MHC-II HLA-DR1 clearly shows disruption of key ionic and hydrophobic interactions necessary for forming the complex. Extensive dislocation of the disulfide loop in particular interferes with MHC-IIα binding. The triple-mutant structure provides new insights into the loss of superantigenicity and toxicity of an engineered superantigen and provides a basis for further design of enterotoxin vaccines.

Keywords: Enterotoxin; major histocompatibility complex; *Staphylococcus aureus*; vaccine design; X-ray structure

Multidrug resistant strains of *Staphylococcus aureus* present a serious worldwide health threat for both immunocompromised patients and immunocompetent people. *S. aureus* strains have developed resistance to penicillin and methicillin (Neu 1992; Michel and Gutmann 1997) and now the recurrent emergence of vancomycin-resistant strains (French 1998; Gilmore and Hoch 1999) threaten the efficacy of all antibiotics in clinical use. Methicillin-resistant *S. aureus* is now the primary cause of nosocomial infections and has lead to drastically increased morbidity and mortality rates in recent years (Ehlert 1999).

Staphylococcus bacteria infect their hosts opportunistically and cause pathology by expressing a number of protein toxins and other virulence factors. The protein toxins are responsible for a number of diseases, such as food poisoning, skin infections, bacterial arthritis, Kawasaki syndrome, rheumatic fever, and toxic shock syndrome (Scherer et al. 1993; Schlievert 1993).

The most well-characterized, structurally and immunologically, *S. aureus* toxins are the staphylococcal enterotoxins (SEs), which are single-chain proteins (23–29 kD) subdivided into serotypes A, B, C1, C2, C3, D, E, G, and H (Marrack and Kappler 1990; Fleischer et al. 1995). SEs are superantigens and as such have the ability to stimulate whole T-cell subpopulations by cross-linking T-cell receptors (TCRs) with MHC-II molecules independent of the antigenic specificity of particular T-cells (Herman et al. 1991).

Reprint requests to: Dr. Bernhard Rupp, Macromolecular Crystallography and Structural Genomics, Lawrence Livermore National Laboratory, LLNL-BBRP, POB 808, L-448, University of California; Livermore, CA 94551, USA; e-mail: br@llnl.gov; fax: (925) 424-3130.

[4]These authors contributed equally to this work.

Article and publication are at http://www.proteinscience.org/cgi/doi/10.1110/ps.39702.

When acting as superantigens, SEs are not processed into smaller peptides for presentation by MHC-II but interact with MHC-II and TCR molecules as intact toxins (Scherer et al. 1993). Previous studies have revealed that TCRs are principally bound by SEs via hydrogen-bond interactions with the main-chain nitrogens and carbonyl oxygens of the ligand-recognition variable loops (CDR2 and HVR4) and via interactions with framework regions of the TCRβ subunit variable domain (Vβ; Choi et al. 1990; Fields et al. 1996).

SEs bind monovalently or bivalently to MHC-II molecules (Abramsen et al. 1995, Tiedemann et al. 1995). Some monovalent SEs (SEB, toxic shock syndrome toxin-1 [TSST-1]) bind exclusively to the conserved α-chain site (or low-affinity site), located outside the conventional peptide antigen-binding groove (Dellabona et al. 1990; Jardetzky et al. 1994; Kim et al. 1994), disrupting contacts between TCR and the MHC-bound peptide (Fields et al. 1996). Other monovalent superantigens (streptococcal pyrogenic exotoxin-C (SPE-C), for example) form contacts with the MHC-bound peptide and the polymorphic β chain of MHC (Hudson et al. 1995; Abramsen et al. 1995) through a zinc-dependent site (or high-affinity site). Staphylococcal enterotoxin A (SEA), one of the most potent T-cell mitogens known, is a bivalent SE, as shown by mutagenesis and binding studies (Abramsen et al. 1995), interacting with MHC-II at both zinc-dependent and zinc-independent sites. The MHC-IIα-binding region, located near the N terminus on SEA (9–12), is homologous to the MHC-IIα binding site of SEB (Jardetzky et al. 1994); whereas, the C-terminal residues H187, H225, and D227 of SEA mediate zinc-dependent binding to H81 of the MHC-IIβ through a tetrahedrally coordinating zinc (Abramsen et al. 1995; Hudson et al. 1995). Tiedemann et al. (1995) were able to isolate HLA-DR·$(SEA)_2$ hetero-trimers in solution and suggest SEA cross-links to two MHC-II molecules on the surface of antigen-presenting cells (Mehindate et al. 1995; Tiedemann et al. 1995, 1996). Kozono et al. (1995) proposed the formation of larger daisy-chain oligomers because the two binding sites do not appear to be competing. Studying the interaction of SEA mutants with either binding site disrupted (double-mutant H187A and H225A and triple-mutant F47S, L48S, and Y92A) with cell surface MHC-II, Tiedemann et al. (1996) concluded that both the high-affinity and low-affinity sites are required for superantigen function. They further proposed $(MHC\text{-}II)_2$·SEA formation is sufficient to induce cytokine production and may be sufficient to initiate a nonspecific T-cell response.

In contrast, the standard model of superantigen toxicity involves the formation of an MHC/TCR/superantigen complex, which circumvents the normal antigen-specific T-cell recognition (Dowd et al. 1995) but leads to nonspecific T-cell activation. SEs stimulate large fractions of whole T-cell populations (Kappler et al. 1992) by interaction with multiple subtypes of V_β subunits. The result is a polyclonal T-cell response of significantly greater magnitude than normal, antigen-specific, activation. Alhough $(MHC\text{-}II)_2$·SEA formation alone might be sufficient to cause cytokine production and T-cell stimulation, recent results (R.G. Ulrich, unpubl.) suggest that T-cell stimulation by SEA is likely to require engagement of the TCR by MHC-II-bound superantigen. By inducing massive T-cell proliferation, SEA causes the release of pathological levels of mast cell leukotrienes and proinflammatory cytokines, which is the basis of SEA's induced toxic shock syndrome (Stiles et al. 1993; Carlsson and Sjogren 1996).

Due to the growing threat from multi-drug-resistant *S. aureus*, efforts have been undertaken to create alternatives to antibiotic treatment for *S. aureus*-caused diseases. A highly promising approach is the development of vaccines against *S. aureus* infections based on the structure of superantigenic SE (Ulrich et al. 1998). SEA with mutations at the DRα-binding site can no longer form MHC-II/TCR/SEA or $(MHC\text{-}II)_2$·SEA complexes and therefore superantigen T-cell stimulation is prevented. Only conventional immune responses from processing and presenting of SEA-derived peptides to T-cells is then observed (Bavari et al. 1996). An engineered SEA triple mutant has been shown to trigger an efficient antibody response and has been shown to vaccinate mice and rhesus monkeys against SEA-triggered septicemia and death (Nilsson et al. 1999). In addition, antibodies produced against one SE vaccine cross-react with other SEs and superantigens by recognizing common structural epitopes. This cross-reactivity makes SE-based superantigen vaccines powerful tools in the fight against *S. aureus* infection and sepsis.

To explore the molecular basis of superantigen vaccine function, we have determined the structure of a nontoxic SEA triple mutant (L48R, D70R, and Y92A). Exploiting the common structural motifs between SEA and SEB MHC-II binding sites (Ulrich et al. 1995), homology models for both wild-type SEA and SEA triple-mutant complexes with MHC-II have been developed. These models provide key insights into altered behavior and loss of MHC-IIα-chain binding and will provide for better rational vaccine design.

Results

Previous studies have shown that a single-site mutation, Y92A, in SEA retained only 10% MHC-II binding (Bavari et al. 1996). Binding assays for the SEA triple-mutant Y92A, L48R, and D70R, with HLA-DR1 revealed further reduced binding to only 1%, compared to wild-type SEA (Fig. 1A). In cellular assays, the SEA triple mutant has highly attenuated biological activity (10^6 reduction, Fig. 1B). The structure of the SEA triple mutant was determined to 1.5 Å by molecular replacement (initial *R*-value of 0.45 and correlation coefficient of 0.56). The modeled structure

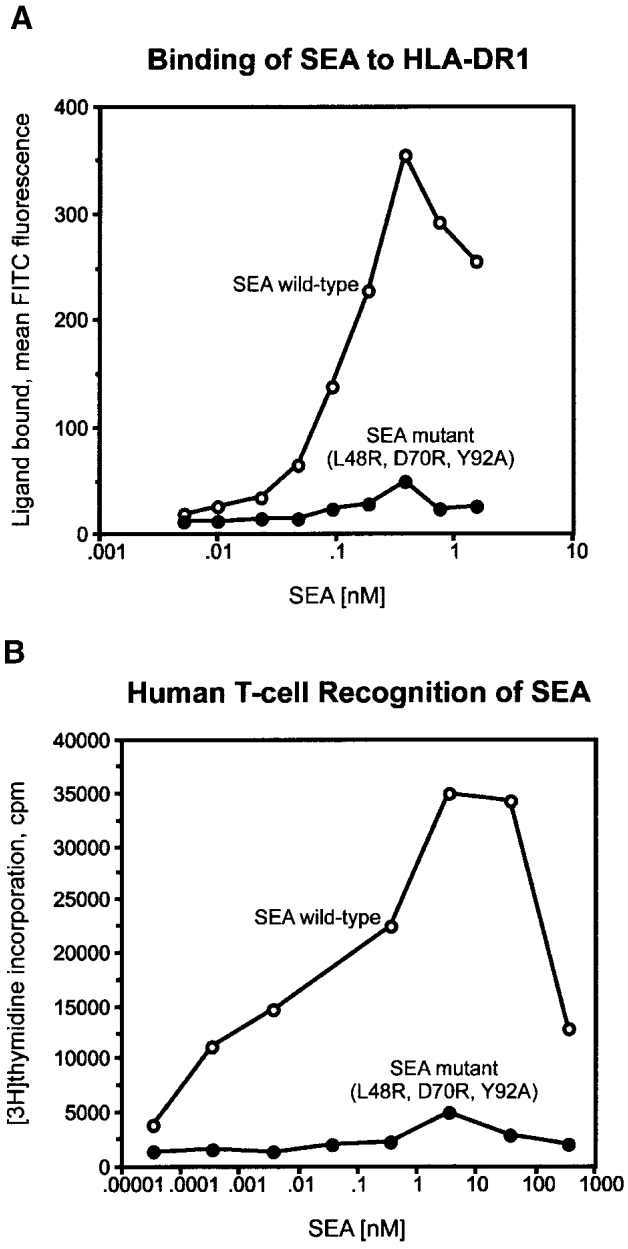

Fig. 1. (*A*) Binding of staphylococcal enterotoxin A (SEA) to HLA-DR1. SEA wild-type is depicted as open circles; the triple-mutant SEA is depicted with solid circles. Binding was tested by subsequently incubating human B-lymphoblastoid cells (LG2) with wild-type or mutant SEA, rabbit anti-SEA, and FITC-labeled goat anti-rabbit IgG. Data shown are representative of three experiments. (*B*) Human T-cell recognition of SEA.SEA wild-type is represented by open circles, mutant SEA by solid circles. Human peripheral blood mononuclear cells were cultured with wild-type or mutant SEA, pulsed-labeled with 1μCi [3H]-thymidine, and finally the incorporation of [3H]-thymidine into the cellular DNA was measured. Data shown are mean values of triplicate determination and are representative of five experiments.

contains residues 6–233 of the expressed construct, a total of 496 water molecules, one Zn^{2+} and one sulfate ion. The final structure was refined to a crystallographic *R*-value of 19.1% (*R*-free = 23.6 %) and has good geometry (Table 1). The structure has been deposited in the Protein Data Bank (PDB; accession code 1DYQ).

Table 1. *Data collection and refinement*

Space group	$P2_12_12_1$
Unit cell dimensions (Å)	a = 39.05, b = 78.65, c = 86.37
Wavelength (Å)	1.1000
Resolution (Å)	1.150
No. observed reflections	158,285 (2,752)[a]
No. unique reflections	35,972 (1,143)[a]
Completeness (%)	82.84 (37.2)[a]
$\langle I/\sigma_{(I)}\rangle$	7.7 (3.4)[a]
R_{sym}[b](%)	6.2 (13.5)[a]
R-value[c](%)	19.1
R_{free}[d] *(%)*	23.6
Average *B* factor[e] (Å^2)	20.0
RMS deviations from ideality[f]	
Bond lengths (Å)	0.016
Bond angles (°)	2.069
Overall coordinate error (R_{free})[g] (Å)	0.063 (0.101)

[a]Values in brackets refer to the highest resolution bin (1.54–1.50 Å).
[b]$R_{sym} = \Sigma\,\Sigma I_{hj} < I_h > /\Sigma\,\Sigma I_{hj}$.
[c]$R = \Sigma\, F_O - F_C/\Sigma F_O$.
[d]R_{free} was calculated using 5% of reflections excluded from refinement (Brünger 1992b).
[e]Wilson plot (Blundell and Johnson 1976).
[f]Calculated with WHATCHECK (Hooft et al. 1996).
[g]Estimated Standard Uncertainty, Diffraction Precision Index (DPI) based on R_{free} (Cruickshank 1999).

Quality of the structure

Model bias was minimized by using *Shake*&wARP (Segelke et al. 2000), a modified wARP procedure (Perrakis et al. 1997), and using maximum-likelihood refinement (REFMAC; Murshudov et al. 1997). WHATCHECK (Hooft et al. 1996) analysis of the agreement between observed and expected bond lengths, bond angles, and stereochemistry gives values in the expected range or better (Table 1). Real-space fit correlation (CCP4 1994) of the model against the electron density reveals an average correlation coefficient of 0.88. Lower correlations were found around residues 50, 100, 162, 190, and 212, mainly corresponding to weak density in solvent-exposed loop regions. The Ramachandran plot (Ramachandran et al. 1963) shows 88.8% of all residues in the most-favored and 11.2% in additional-allowed regions; none have disallowed conformations.

The final $wF_o\phi_c$ *Shake*&wARP electron density map is continous for the whole polypeptide backbone for residues 6–233 and very well defined for 96% of the amino acid residues. Residues 190 and 191 have poorly defined electron densities due to variable conformations. Side chains of surface exposed residues E9, K41, D60, K74, and E191 are only partly defined.

Structural comparison to wild-type SEA

The overall topology of the SEA triple mutant closely resembles that of the native protein (Schad et al. 1995), folding into two domains (domain I, residues 31–116, and β-barrel domain II, residues 117–233). Domain II also includes the N-terminal segment 6–30. Introduction of three point mutations—L48R, D70R, and Y92A—(Ulrich et al. 1995; Bavari et al. 1996) leads to formation of a bifurcated sheet sharing β1 and β4a strands in domain I (nomenclature derived from Schad et al. 1995).

The C_α backbone of the mutant structure superimposes closely with wild-type SEA (rmsd of 0.53 Å for 199 C_α, excluding residues 11–47, 51–59, 64–92, 103–200, and 208–233), although mutations have caused notable alterations to some loops (Fig. 2). Rmsd is 1.71 Å for all C_α in common between the wild-type and mutant SEA. The most significant structure deviations occur in three regions known to be involved in formation of a complex with HLA-DR1α: between residue D45–T51, residue Y91–A105, and residue L198-L210. Residues 45–51 are located between β strands β1 and β2, forming a large reverse turn connecting the bifurcated sheets. The engineered R48 is situated at the outermost turn of this loop, causing its neighboring residues F47 and E49 to shift substantially from their native position (1.54 Å and 3.13 Å, respectively, on C_α). R48 also forms a hydrogen bond (2.78 Å) with G98 backbone carbonyl in the adjacent loop.

The region between residues 91–105 is referred to as the disulfide loop. It contains the C terminus of β strand β4a, a 3_{10}-helix (G93-C96), a seven-residue-long loop and the N terminus of β strand β5a. The substitution Y92A at the N terminus of β strand β4a results in a slightly extended strand. The disulfide loop is held in place by the conserved disulfide bond between C96 and C106 found in all SEs. Interestingly, C96 in the native SEA structure is part of the C-terminal end of β strand β4b; whereas, in the mutant, C96 forms part of a 3_{10}-helix (G93-C96) just behind the engineered Y92A mutation. As part of the 3_{10}-helix the C_α of C96 is moved 2.20 Å from its original position in the native structure, altering location and conformation of the disulfide bond. These movements and the formation of additional hydrogen bonds due to the point mutations L48R and D70R (H-bonds to G98O [2.78 Å] and Q95O [3.02 Å], respectively) are the likely cause of the loop region (91–105) flip into a solvent exposed orientation (Fig. 2). Stabilization of this dislocated loop is achieved by 3_{10}-helix formation, with residues Y94 and Q95 now oriented toward the inside of the molecule, altering the locations of their functional groups by 12 Å from the wild-type structure. Because the reverse turn and the disulfide loop both participate in connections between the β strands (β1–β2 and β4a–5a) of the bifurcated sheet, the formation of this structural element is most probably induced by the engineered mutations. The nearby loop 45–51 is involved in crystal packing interactions (Q49 h-bonds with E28 and S206 of a symmetry related molecule); however, these interactions are unlikely to influence the conformation of the disulphide loop (91–105). Whereas in region 45–51, four potential hydrogen bonds of E49 with adjoining molecules were found; there were no crystal-packing interactions observed with symmetry-related mol-

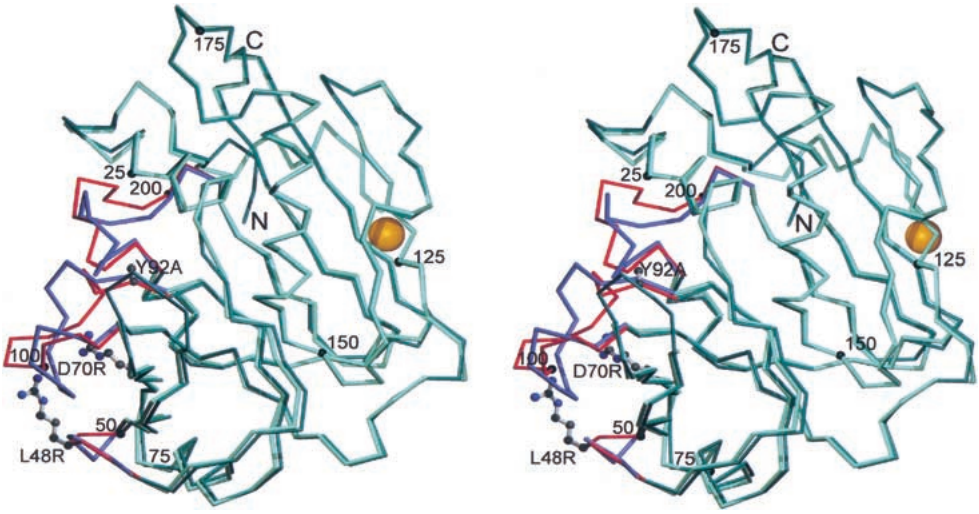

Fig. 2. Stereo C_α-backbone diagrams of the SEA triple mutant, shown in dark green, superimposed with native SEA, depicted in green (rmsd = 0.53 Å; 199 C_α atoms aligned). Structure deviations occur in three loop regions, harboring the engineered mutations, which are highlighted in red and blue for the mutant and the wild-type SEA, respectively. The engineered point mutations L48R, D70R, and Y92A are shown as ball-and-stick representations, color-coded according to atom type. Every twenty-fifth Cα of wild-type SEA is labeled and represented as a black sphere. The zinc ion of SEA mutant is shown as a cpk-representation in orange.

ecules that might influence the conformation of the disulfide loop (91–105).

Finally, major structural deviations occur in domain II, in region 198–210, representing an expanded loop from L198 to Y205 and the five N-terminal residues of α-helix α5. Whereas Y94 and Q95 are entirely solvent exposed in native SEA, they are oriented toward the core of the molecule and more buried in the mutant. Relocation of this loop is mainly stabilized by hydrophobic interactions because the greatest effects are found around G203 and Y205, located at the loop turning points, which are shifted 4.66 Å and 3.08 Å, respectively, from their native C_α positions (Fig. 2). Crystal-packing interactions with symmetry-related molecules observed within proximity of the altered loop region 198–210 are rather weak, partly due to their location at the end of the region, and are unlikely to significantly determine the conformation of this loop.

Discussion

Available crystal structures of SEs and their complexes provide a detailed understanding of SE interactions with MHC-II and TCR molecules. The SEA triple mutant clearly shows attenuated binding affinity to HLA-DR1 molecules (Fig. 1A), as well as greatly reduced biological activity (Fig. 1B). The structural study of an inactive SEA triple mutant gives insight into detailed molecular changes that result in attenuated binding and biological activity and provides important insight for structural-based rational design of other SE and superantigen vaccines.

Homology models of ternary complexes

Similarity between SEA, SEB, and SPE-C and the availability of crystal structures of SEB and SPE-C complexes with MHC-II and TCR molecules (Jardetzky et al. 1994; Li et al. 1998; Li et al. 2001) make it possible to construct a hypothetical SEA·TCR·$(MHC\text{-}II)_2$ quaternary complex.

SEA and SEB are known to compete for binding to MHC-II molecules, indicating analogous binding mechanism and location at least at one binding site (Schad et al. 1995). Furthermore, SEA and SEB share 31% sequence homology (36% identity over 229 aligned C_α atoms; rmsd 2.0 Å) and hence highly similar folds. β-barrel and β-grasp motifs (four-stranded mixed β sheet with an α-helix packed across one face of the sheet; Overington 1992) are present in both structures. The C_α alignment of wild-type SEA with the SEB (rmsd 2.0 Å) reveals differences primarily in the SEA N terminus, in loops of low-sequence homology, and in the disulfide-loop region (A90-V111; Ulrich et al. 1995). The recent publication of the SPE-C/MHC-II complex provides a basis for modeling the zinc-dependent interaction between SEA and MHC-IIβ (Li et al. 2001). SEA and SPE-C bind the MHC-IIβ chain similarly at the high-affinity binding site, contacting N-terminal residues of bound peptide.

The quaternary SEA·TCR·$(MHC\text{-}II)_2$ (Fig. 3) is built by C_α alignment of SEA in the modeled ternary complex with the SPE-C in the MHC-IIα complex (Li et al. 2001). From the putative quaternary complex it appears the engineered mutations of the vaccine would have no effect on TCR binding and MHC-II binding at the zinc-dependent site. The binding regions that interact with MHC-IIα at the zinc-independent site are significantly altered however.

Binding interface with MHC-II (HLA-DR1)α chain

SEB/HLA-DR1α complex

In the crystal structure of the SEB/HLA-DR1α complex, most intermolecular interactions occur in three loop regions: residues 44–50 (reverse turn), residues 90–111 (disulfide-loop region), and residues 200–212 (Fig. 4A). The reverse turn and the disulfide-loop region form a deep binding pocket composed of a hydrophobic ridge (F44, L45, and F47) and a polar groove derived from three β strands of the β-grasp motifs in domain II. Residue E67 at the base of the polar pocket forms a salt bridge with K39 of the DRα subunit. Additionally, SEB residues Y89 and Y115 form two hydrogen bonds with DRα-K39 (Fig. 4A). In three different SEB mutants, the substitutions E67Q, Y89A, and Y115A each reduced DRα binding by 100-fold (Ulrich et al. 1995), emphasizing the key role of these anchoring residues. The SEB disulfide loop interacts with the α-helix from the DR1α domain through residues 92–96, most significantly by Y94 (Jardetzky et al. 1994). The third loop region (200–212) contacts the DR1 molecule at the C-terminal end of the DR1α-helix mainly through hydrogen bonds involving residues 210–212 (Jardetzky et al. 1994).

SEA/HLA-DR1α complex

From the modeled complex of SEA with HLA-DR1, it is clear that the main SE-MHC interactions at the DRα site are conserved, as compared with SEB·HLA-DR1α (Fig. 4B). The three loop regions involved in complex formation of SEA with HLA-DR1α are D45–T51, Y91–A105 (disulfide loop), and L198–L210. Residues E67, Y89, and Y115 of the SEB-binding interface correspond to D70, Y92, and Y108 in SEA. Mutation of the SEA key residue Y92A resulted in 100-fold reduced HLA-DR1α; the single-site mutation Y108A has negligible effect on binding (Ulrich et al. 1995), although the homologous substitution in SEB (Y115A) has a substantial effect. The substitution of SEB E67 with the shorter carboxylate side chain of SEA D70 is thought to increase distances of Y92 and Y108 to DRα-K39 and therefore cause weaker interactions in the native SEA·MHC-II complex. The weaker SEA Y108-DRα K39 interaction makes it easier to accommodate the Y108A substitution.

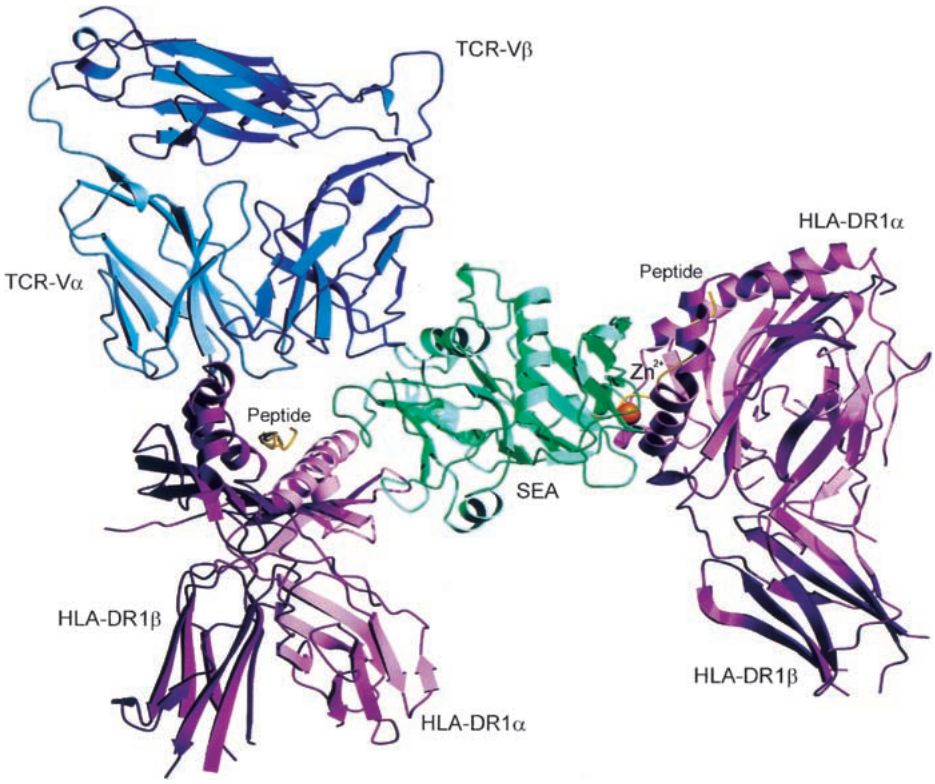

Fig. 3. Molecular homology model of native SEA in complex with two MHC-II (HLA-DR1) molecules and the T-cell receptor (TCR) in ribbon presentation. The model is based on the crystal structures of free SEA (1ESF), complexed HLA-DR1 (1SEB and 1HQR), and complexed TCR (1SSB). SEA is shown in green, with Zn^{2+} as a cpk-representation in orange. The α subunit of HLA-DR1 is depicted in light purple, the β subunit in dark purple. An antigenic peptide molecule bound to the antigen-presenting cleft of a HLA-DR1 molecule is depicted in yellow. Subunits α and β of the TCR are colored light and dark blue, respectively.

Hydrogen bond formation between D70OD2 and α-K39NZ will require α-K39 to shift toward SEA to compensate for the shorter aspartate chain and optimize ion-pair interactions.

Engineered mutations disrupt binding

In vaccine design, SEA residues that primarily mediate HLA-DRα binding have been targeted to produce a vaccine devoid of pathological activity. The point mutations D70R and Y92A were engineered in the presented SEA triple mutant, accompanied by a mutation L48R added as a safety factor (Ulrich et al. 1998).

The D70R substitution leads to the disruption of the DRα-K39 salt bridge, one of the key interactions in DRα binding. Replacing the original aspartate by the bulkier and oppositely charged arginine causes both steric and charge repulsion (distance R70NH1–α-K39NZ 1.23 Å). Further destabilization of interactions with HLA-DRα is achieved by the Y92A substitution. Due to the loss of a hydrogen bond acceptor and the large shift of residue 92 (10.3 Å) away from its position in the native structure, a potential hydrogen bond with DRα-K39 is eliminated. Only one intermolecular H-bond remains between the SEA triple mutant and HLA-DR1 (DRα/K39-SEA/Y108, 2.83 Å). This H-bond, if it forms, is insufficient to initiate or sustain binding with HLA-DR1. Furthermore, substitution D70R results in a new intramolecular hydrogen bond (R70NH1–Q95O, 3.02 Å), stabilizing a conformation that disfavors HLA-DR1 binding.

L48 is found in the hydrophobic reverse turn and represents the only absolutely conserved residue in all bacterial superantigens (Ulrich et al. 1995) and L48 is essential for initial binding of MHC-II molecules. Inserting an arginine in this nonpolar loop introduces a particularly bulky and charged residue, leading to the disruption of the otherwise close fit of this loop into the predominantly hydrophobic groove on the DRα chain (Fig. 4C). Interestingly, besides disrupting important interactions with the HLA-DR1α subunit, the two newly introduced arginines, R 48 and R 70, form an arginine cluster with R 211 and R 214 on the surface of the SEA mutant, preventing access of the MHC-IIα chain by shielding the binding pocket and changing the surface polarity. The new hydrogen bonds formed by R 48 are also responsible for a cascade of structural rearrange-

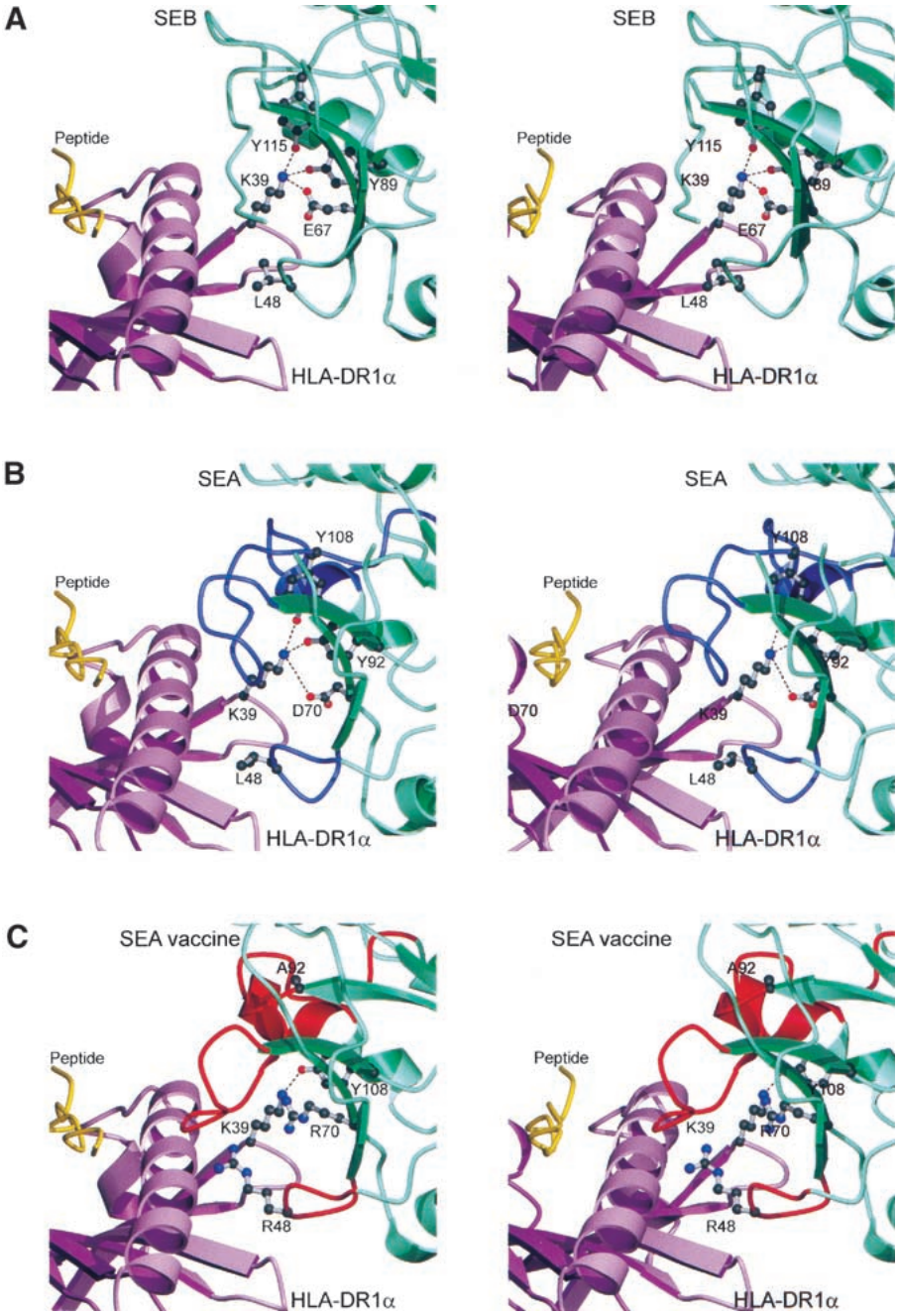

Fig. 4. Binding interface models of staphylococcal enterotoxins (SEs) with HLA-DR1α in ribbon presentation. The HLA-DR1α subunit is depicted in light purple, with the bound peptide molecule shown in yellow. Overall, SEs are presented in green. Key anchoring residues are represented as ball-and-stick models, colored according to atom type. (*A*) Representation of the native SEB/HLA-DR1 complex based on the crystal structure (1SEB). Residue K39 from the DR1α subunit forms a salt bridge with E67 and two hydrogen bonds with Y115 and Y89 from SEB. L48 binds into a hydrophobic groove composed by the three adjacent β-sheets of HLA-DR1α. Loop 88–105 is incomplete due to absent electron density. (*B*) Homology model of the SEA/HLA-DR1 complex based on the crystal structures of native SEA (1ESF) and complexed HLA-DR1 (1SEB). The three loop regions essential for binding the DR1α subunit are highlighted in blue. Residues D70, Y108, and Y92 correspond to the binding residues in SEB. The model shows the same binding mode as SEB, proposing a stable SEA/HLA-DR1 complex. (*C*) Homology model of the SEA triple mutant in proposed complex with HLA-DR1, based on our crystallographic data and complexed HLA-DR1 (1SEB). The three loop regions proposed in binding the DRα subunit are highlighted in red. The engineered point mutations are residues L48R, D70R, and Y92A. Due to the bulkiness and reversed charge of the inserted arginines, as well as the arrangement of the dislocated disulfide loop, which protrudes through the DRα-helix, a zinc-independent binding mode homologous to the native SEA/MHC-IIα/TCR complex, is impossible.

ments, affecting neighboring loop regions. The most striking result is the dislocation of disulfide-loop 91–105 to solvent-exposed orientation (Fig. 4C). The homology model positions the disulfide loop within such a short distance to the DR1 molecule that the loop virtually protrudes through the DRα-helix, suggesting binding of the SEA triple mutant will be substantially disfavored due to strong van der Waals repulsion forces.

Structural basis of vaccine efficacy

Binding assays showing the affinity of the SEA triple mutant for HLA-DR1 indicate a binding reduction of $>10^2$ compared to the wild-type protein (Fig. 1A) and attenuated biological activity of $>10^6$ (Fig. 1B). Discrepancies between apparent receptor-binding affinity and biological activity were noted previously (Leder et al. 1998). It is difficult to account for the substantial loss of binding by mutating the zinc-independent binding site alone, given that the zinc-dependent binding site is apparently unaffected by the engineered mutations. Reduced biological activity and altered SEA/MHC-II-binding stoichiometry would be expected, along with intact zinc-dependent binding. A full explanation of these findings requires further investigation and some zinc-mediated binding to HLA-DR1 cannot be ruled out. Possible binding to the zinc-dependent site in the absence of zinc-dependent site interactions has been shown by Tiedemann et al. (1995). A different triple mutant—F47S, L48S, and Y92A—predicted to exhibit defective interaction with DRα, showed residual binding to cell-surface MHC-II (Tiedemann et al. 1995). Bivalent receptor-binding surfaces of SEA promote cross-linking of MHC-II molecules on the cell surface, increasing biological potency (Tiedemann et al. 1995). Loss of DRα binding is likely to prevent TCR binding in an orientation that is favorable to T-cell stimulation (Ulrich et al. 1995). In the X-ray structure, Zn^{2+} is tetrahedrally complexed by H187, H225, and D227 and H44 of a symmetry-related SEA triple-mutant molecule. H44 is located within the engineered N-terminal-loop region harboring L48R of the SEA mutant. This suggests a possible dimerization of the SEA triple mutant in a head-to-tail arrangement that would block binding at the high-affinity site. Therefore reduced MHC-II binding could be explained even though the zinc-binding site is not directly affected by the engineered mutations. However, the available evidence suggests that the SEA triple mutant is predominately monomeric in solution (Ulrich, unpubl.).

The crystal structure of SEA vaccine provides the structural basis for understanding the loss of superantigenicity in the SEA triple mutant. Consistent with biochemical and cellular assays, the SEA vaccine X-ray structure and the homology model show that the combination of the three mutations L48R, D70R, and Y92A severely disrupts zinc-independent binding of SEA to MHC-II. Without DRα binding, the productive formation of ternary or quaternary complexes is impaired and superantigenic stimulation of T-cells is prevented.

Engineering of a defective zinc-binding site could contribute to further vaccine development, given that SEA-mediated cross-linking requires this site and stimulates T-cell independent release of cytokines, a response also mimicked by antibody-mediated MHC-II cross-linking (Mehindate et al. 1995). However, Fig. 1B shows that disrupting the low-affinity, zinc-independent binding site is sufficient to abolish superantigenicity in SEA. Overall, structural and biomedical data confirm the utility and efficacy of the SEA triple mutant as a potent immunogen and as a safe vaccine. This vaccine may provide immunity to multiple bacterial superantigens because antibodies produced against SEA display cross-reactivity against other SEs. The SEA triple mutant may serve as a model for structure-based rational design of other SE and superantigen vaccines. Facing the increasing threat of multi-antibiotic-resistant *Staphylococcus* strains, a potential superantigen vaccine provides important contributions in the fight against a number of *S. aureus*-triggered human diseases.

Materials and methods

Binding of SEA to HLA-DR

DR1 homozygous, human B-lymphoblastoid cells (LG2) were incubated 40 min (5×10^5 cells; 37°C) with wild-type or mutant SEA in Hanks balanced salt solution (HBSS) containing 0.5% bovine serum albumin. The cells were washed with HBSS and then incubated with 5 μg of affinity-purified rabbit anti-SEA or SEB antibody (Toxin Technology) for 20 min at 4°C. Unbound antibody was removed, and the cells were incubated with FITC-labeled goat anti-rabbit IgG (Organon Teknika Corp.) on ice for 30 min. The cells were washed and analyzed by flow cytometry (FACScan; Becton Dickinson & Co.).

Human T-cell recognition of SEA

Human peripheral blood mononuclear cells were purified by Ficoll-hypaque (Sigma) buoyant density gradient centrifugation and cultured with wild-type or mutant SEA in RPMI-1640 with 5% fetal bovine serum. Following 72 h of culture, the mononuclear cells were pulse-labeled for 12 h with 1μCi [3H]-thymidine (Amersham) and harvested onto glass-fiber filters. Incorporation of [3H]-thymidine into the cellular DNA was measured by liquid scintillation (TopCount; Wallac Inc.).

Protein crystallization, data collection, and processing

The SEA triple mutant was expressed and purified as described previously (Ulrich et al. 1995; Bavari et al. 1996). Crystals were obtained at 4°C by hanging drop vapor diffusion (McPherson 1982) in 8 μL drops (4 μL of the reservoir solution, 10% PEG 6000, 5% MPD, and 0.1 M HEPES at pH 7.8 and 4 μL protein stock solution of 2 mg/mL) suspended over a 1-mL reservoir. X-ray diffraction data were collected with a Quantum4 ADSC CCD detector from a single cryo-cooled crystal (Oxford Cryosys-

tems) on Advanced Light Source (ALS) beamline 5.0.2 at $\lambda = 1.1000$ Å. A total of 130 images were collected with an oscillation range of 1°. Crystals were diffracted to 1.5 Å. The crystal belonged to space group $P2_12_12_1$ with the unit cell parameters $a = 39.05$, $b = 78.65$, and $c = 86.37$ Å. Calculation of V_m (Matthews 1968) indicated one molecule in the asymmetric unit ($V_m = 2.62$ Å^3/Da) and an approximate solvent content of 52%. The data were indexed and integrated with MOSFLM (CCP4 1994) and scaled with SCALA and TRUNCATE from the CCP4 program suite (CCP4 1994).

Structure determination and refinement

The structure was solved by molecular replacement using EPMR (Kissinger et al. 1999) with native SEA (1ESF; Schad et al. 1995) as a search model (minus cadmium ion). Initial maps were generated with *Shake*&wARP (Segelke et al. 2000), a modified version of wARP (Perrakis et al. 1997), in combination with REFMAC unrestrained maximum-likelihood minimization (Murshudov et al. 1997). Model building was performed with XtalView (McRee 1992) using the wild-type SEA structure as a template. Solvent structure was built by manual placement and by iteratively using ARP (Lamzin and Wilson 1993) and REFMAC (Murshudov et al. 1997). Further refinement was carried out with REFMAC and Xplor (Brünger 1992a) and included bulk solvent correction, overall anisotropic B-factors, rigid body refinement, prepstage, group B-factor, and final individual B-factor refinement.

Structural analysis and homology models

Sequence alignments were performed with BLAST search (Altschul et al. 1997); structure alignments were performed with the DALI server (Holm and Sander 1996). Homology models were developed using X-ray coordinate data from the following PDB files: 1ESF, 1SEB, 1SBB, 1HQR, and 1AO7 (Jardetzky et al. 1994; Schad et al. 1995; Garboczi et al. 1996; Li et al. 1998, 2001). Superposition of molecules and rmsd calculation were done with the program Midas (Ferrin et al. 1988).

Figures

Secondary structure assigned according to Kabsch and Sander (1983). Figures were drawn with MOLSCRIPT (Kraulis 1991) version 2.1.2 using the POVSCRIPT patch (copyright Dan Peisach) and rendered with POV-Ray (Persistance of Vision Raytracer, v.3.1g, 1999).

Acknowledgments

We thank P. Hoechtl and M. Forstner for help with data collection and contributions to structure determination. X-ray diffraction data were collected at the Advanced Light Source Beam Line 5.0.2. A.L.S. is supported by the Director, Office of Science, Office of Basic Energy Sciences, Materials Sciences Division, of the U.S. Department of Energy (DOE) under contract no. DE-AC03–76SF00098 at Lawrence Berkeley National Laboratory. This work was carried out under the auspices of the U.S. Department of Energy (DOE) by Lawrence Livermore National Laboratory under contract no. W-7405-ENG-48.

The publication costs of this article were defrayed in part by payment of page charges. This article must therefore be hereby marked "advertisement" in accordance with 18 USC section 1734 solely to indicate this fact.

References

Abramsen, L., Dohlsten, M., Segren, S., Björk, Jonsson, E., and Kalland, T. 1995. Characterization of two distinct MHC class II binding sites in the superantigen staphylococcal enterotoxin A. *EMBO J.* **14:** 2978–2986.

Altschul, S.F., Madden T.L., Schaffer A.A., Zhang J., Zhang Z., Miller W., and Lipman D.J. 1997. Gapped BLAST and PSI-BLAST: A new generation of protein database search programs. *Nucleic Acids Res.* **25:** 3389–3402.

Bavari, S., Dyas, B., and Ulrich R.G. 1996. Superantigen vaccines: A comparative study of genetically attenuated receptor-binding mutants of staphylococcal enterotoxin A. *J. Infect. Dis.* **174:** 338–345.

Brünger, A. 1992a. T. *X-PLOR, Version 3.1. A system for X-ray crystallography and NMR.* Yale UniversityPress, New Haven, CT.

Brünger, A. 1992b. T. Free R-value: A novel statistical quantity for assessing the accuracy of crystal structures. *Nature* **355:** 472–475.

Carlsson, R. and Sjogren, H.O. 1996. Kinetics of IL-2 and interferon-γ production, expression of IL-2 receptors, and cell proliferation in human mononuclear cells exposed to staphylococcal enterotoxin A. *Cell. Immunol.* **96:** 175–183.

CCP4 (Collaborative Computational Project Number 4). 1994. The CCP4 suite: Programs for protein crystallography. *Acta Crystallogr.* **D55:** 484–491.

Choi, Y., Herman, A., DiGiusto, D., Wade, T., Marrack, P., and Kappler, J. 1990. Residues of the variable region of the T-cell-receptor β-chain that interact with *S. aureus* toxin superantigens. *Nature* **346:** 471–473.

Cruickshank, D.W.J. 1999. Remarks about protein structure precision. *Acta Crystallogr.* **D55:** 583–601.

Dellabona, P., Peccoud, J., Kappler, J., Marrack, P. Benoist, C., and Mathis, D. 1990. Superantigens interact with MHC class II molecules outside of the antigen groove. *Cell* **62:** 1115–1121.

Dowd, J.E., Jenkins, R.N., and Karp, D.R. 1995. Inhibition of antigen-specific T cell activation by staphylococcal enterotoxins. *J. Immunol.* **154:** 1024–1031.

Ehlert, K. 1999. Methicillin-resistance in *Staphylococcus aureus*—Molecular basis, novel targets and antibiotic therapy. *Curr. Pharm. Des.* **5:** 45–55.

Ferrin, T.E., Huang, C.C., Jarvis, L.E., and Langridge, R. 1988. The MIDAS Display System. *J. Mol. Graph.* **6:** 13–27.

Fields, B.A., Malchiodi, E.L., Li, H., Ysern, X., Stauffacher, C., Schlievert, P.M., Karjalainen, K., and Mariuzza, R.A. 1996. Crystal structure of a T-cell receptor β-chain complexed with a superantigen. *Nature* **384:** 188–192.

Fleischer, B., Gerlach, D., Fuhrmann, A., and Schmidt, K.H. 1995. Superantigens and pseudosuperantigens of gram-positive cocci. *Med. Microbiol. Immunol.* **184:** 1–8.

French, G.L. 1998. Enterococci and vancomycin resistance. *Clin. Inf. Dis.* **27:** 75–83.

Garboczi, D.N., Ghosh, P., Utz, U., Fan, Q.R., Biddison, W.E., and Wiley, D.C. 1996. Structure of the complex between human T-cell receptor, viral peptide and HLA-A2. *Nature* **384:** 134–141.

Gilmore, M.S. and Hoch, J.A. 1999. Antibiotic resistance. A vancomycin surprise. *Nature* **399:** 525–527.

Herman, A., Kappler, J.W., Marrack, P., and Pullen A.M. 1991. Superantigens: Mechanism of T-cell stimulation and role in immune responses. *Annu. Rev. Immunol.* **9:** 745–772.

Holm, L. and Sander, C. 1996. Mapping the protein universe. *Science* **273:** 595–660.

Hooft, R.W.W., Vried, G., Sander, C., and Abola, E.E. 1996. Errors in protein structures. *Nature* **381:** 272.

Hudson, K.R, Tiedemann, R.E., Urban, R.G., Lowe, S.C., Stominger, J.L., and Fraser, J.D. 1995. Staphylococcal enterotoxin A has two cooperative binding sites on major histocompatibility complex class II. *J. Exp. Med.* **182:** 711–720.

Jardetzky, T.S., Brown, J.H., Gorga, J.C., Stern, L.J., Urban, R.G., Chi, Y., Stauffacher, C., Stominger, J.L., and Wiley, D.C. 1994. Three-dimensional structure of a human class II histocompatibility molecule complexed with superantigen. *Nature* **368:** 711–718.

Kabsch, W. and Sander, C. 1983. Dictionary of protein secondary structure: Pattern recognition of hydrogen-bonded and geometrical features. *Biopolymers* **22:** 2577–2637.

Kappler, J., Kotzin, B., Herron L., Gelfand, E.W., Bigler, R.D., Boylston, A., Carrel, S., Posnett, D.N., Choi, Y., and Marrack, P. 1992. V β-specific

stimulation of human T cells by staphylococcal toxins. *Science* **244:** 811–813.

Kim, J., Urban, R.G., Strominger, J.L., and Wiley, D.C. 1994. Toxic shock syndrome toxin-1 complexed with a class II major histocompatibility molecule HLA-DR1. *Science* **266:** 1870–1874.

Kissinger, C.R., Gehlhaar, D.K., and Fogel, D.B. 1999. Rapid automated molecular replacement by evolutionary search. *Acta Crystallogr*. **D55:** 484–491.

Kozono, H., Parker, D., White, J., Marrack, P., and Kappler, J. 1995. Multiple binding sites for bacterial superantigens on soluble class II MHC molecules. *Immunity* **3:** 187–196.

Kraulis, P.J. 1991. MOLSCRIPT: A program to produce both detailed and schematic plots of protein structures. *J. Appl. Crystallogr.* **24:** 916–924.

Lamzin, V.S. and Wilson, K.S. 1993. Automated refinement of protein models. *Acta Crystallogr*. **D49:** 129–147.

Leder, L., Llera, A., Lavoie, P.M., Lebedeva, M.I., Li, H., Sekaly, R.P., Bohach, G.A., Gahr, P.J., Schlievert, P.M., Karjalainen, K., and Mariuzza, R.A. 1998. A mutational analysis of the binding of staphylococcal enterotoxins B and C3 to the TCR β chain and major histocompatibility complex class II. *J. Exp. Med.* **187:** 823–33.

Li, H., Llera, A., Tsuchiya, D., Leder, L., Ysern, X., Schlievert, P.M., Karjalainen, K., and Mariuzza, R.A. 1998. Three-dimensional structure of the complex between a T-cell receptor β chain and the superantigen staphylococcal enterotoxins B. *Immunity* **9:** 807–816.

Li, Y., Li, H., Dimasi, N., McCormick, J.K., Martin, R., Schuck, P., Schlievert, P.M., and Mariuzza, R.A. 2001. Crystal structure of a superantigen bound to the high-affinity, zinc-dependent site on MHC Class. *Immunity* **14:** 93–104.

Marrack, P. and Kappler, J. 1990. The staphylococcal enterotoxins and their relatives. *Science* **248:** 705–711.

Matthews, B.W. 1968. Solvent content of protein crystals. *J. Mol. Biol.* **33:** 491–497.

McPherson, A. 1982. *Preparation and analysis of protein crystals*. John Wiley and Sons, New York, p. 96.

McRee, D.E. 1992. A visual protein crystallographic software system for X11/Xview. *J. Mol. Graph.* **10:** 44–46.

Mehindate, K., Thibodeau, T., Dohlsten, M., Kalland, T., Sékaly, R.-P., and Mourad, W. 1995. Cross-linking of major histocompatibility complex class II molecules by staphylococcal enterotoxin A superantigen is a requirement for inflammatory cytokine gene expression. *J. Exp. Med.* **182:** 1573–1577.

Michel, M. and Gutmann, L. 1997. Methicillin-resistant *Staphylococcus aureus* and vancomycin-resistant enterococci: Therapeutic realities and possibilities. *Lancet* **349:** 1901–1906.

Murshudov, G.N., Vagin, A.A., and Dodson. E.J. 1997. Refinement of macromolecular structures by the maximum-likelihood. *Acta Crystallogr*. **D53:** 240–255.

Neu, H.C. 1992. The crisis in antibiotic resistance. *Science* **257:** 1064–1073.

Nilsson, I.-M., Verdreng, M., Ulrich, R.G., Bavari, S., and Tarkowski, A. 1999. Protection against *Staphylococcus aureus* sepsis by vaccination with recombinant staphylococcal enterotoxin A devoid of superantigenicity. *J. Infect. Dis.* **180:** 1370–1373.

Overington, J.P. 1992. Comparison of three-dimensional structures of homologous proteins. *Curr. Opin. Struct. Biol.* **2:** 394–401.

Perrakis, A., Sixma, T.K., Wilson, K.S., and Lamzin, V.S. 1997. wARP: Improvement and extension of crystallographic phases by weighted averaging of multiple-refined dummy atomic models. *Acta Crystallogr*. **D53:** 448–455.

Ramachandran, G.N., Ramakrishnan, C., and Sasisekharan, V. 1963. Stereochemistry of polypeptide chain configurations. *J. Mol. Biol.* **7:** 95–99.

Schad, E.M., Zaitseva, I., Zaitsev, V.N., Dohlsten, M., Kalland, T., Schlievert, P.M., Ohlendorf, D.H., and Svenson, L.A. 1995. Crystal structure of the superantigen staphylococcal enterotoxin type A. *EMBO J.* **14:** 3292–3301.

Scherer, M.T., Ignatowicz, L., Winslow, G., Kappler, J., and Marrack, P. 1993. Superantigens: Bacterial and viral proteins that manipulate the immune system. *Annu. Rev. Cell Biol.* **9:** 101–128.

Schlievert, P.M. 1993. Role of superantigens in human disease. *J. Infect. Dis.* **167:** 997–1002.

Segelke, B.W., Forstner, M., Knapp, M., Trakhanov, S.D., Parkin, S., Newhouse, Y.M., Bellamy, H.D., Weisgraber, K.H., and Rupp, B. 2000. Conformational flexibility in the apolipoprotein E amino-terminal domain structure determined from three new crystal forms: Implications for lipid binding. *Protein Sci.* **9:** 886–897.

Stiles, B.G., Bavari, S., Krakauer, T., and Ulrich, R.G. 1993. Toxicity of staphylococcal enterotoxins potentiated by lipopolysaccaride: Major histocompatibility complex class II molecule dependency and cytokine release. *Infect. Immun.* **61:** 5333–5338.

Tiedemann, R.E. and Fraser, J.D. 1996. Cross-linking of MHC class II molecules by staphylococcal enterotoxin A is essential for antigen-presenting cell and T cell activation. *J. Immunol.* **157:** 3958–3966.

Tiedemann, R.E., Urban, R.J., Strominger, J.L., and Fraser, J.D. 1995. Isolation of HLA-DR1·(staphylococcal enterotoxin A)$_2$ trimers in solution. *Proc. Natl. Acad. Sci.* **92:** 12156– 12159.

Ulrich, R.G., Bavari, S., and Olson, M.A. 1995. Staphylococcal enterotoxins A and B share a common structural motif for binding class II major histocompatibility complex molecules. *Nature Struct. Biol.* **2:** 554–560.

Ulrich, R.G., Olson, M.A., and Bavari, S. 1998. Development of engineered vaccines effective against structurally related bacterial superantigens. *Vaccine* **16:** 1857–1864.

Wilson, A.J.C. 1942. Determination of absolute from relative X-ray intensity data. *Nature* **150:** 152.